Catalogue of far-infrared measurements of compact galaxies obtained in sparse-map mode with ISOPHOT

Szilárd Csizmadia, Péter Ábrahám, Attila Moór

Konkoly Observatory
Budapest, Hungary

1-December-2006

Contents

1 Introduction

1.1 Sparse-map observations with ISOPHOT/C100

One observing mode of ISOPHOT, the photometer on-board ESA's *Infrared Space Observatory (ISO)*, was the sparse-map mode, when a chain of measurements was carried out within a three degrees diameter field on the sky (the maximum number of the measurements was limited to 30). The detector was open and was measuring through the whole measurement sequence, even during slews from one position to the next. The sequence started with multifilter observation of a sky position (either a source or a background field), followed by a Fine Calibration Source (FCS) measurement obtained with the last filter in the multifilter sequence. These measurements formed the starting AOT (Astronomical Observing Template) of the sparse map sequence. In the case of the far-infrared cameras of ISOPHOT this AOT was called PHT37. Then typically source and background multifilter measurements alternated, each observation corresponding to a separate AOT PHT38. Finally, the last science observation was followed by another FCS measurement (AOT PHT39). Each sparse map step has its own TDT number which identifies it in the ISO Data Archive.

With the ISOPHOT far-infrared cameras (C100/C200) sparse-map observations were carried out during about 1500 hours. The number of PHT37/38/39 AOTs is 2806, which is about 9% of all ISO measurements. With the C100 camera 1695 sparse-map observations were done observations were produced (including both source and background measurements).

1.2 Compact galaxy sample

In the present work we evaluate a sparse map data set containing far-infrared observations of compact galaxies obtained with the ISOPHOT C100 camera. The sample is consisting of observations proposed by M. Vigotti (observer ID: MVIGOTTI). The total number of measurements is 129 (64 galaxy observations and 65 background fields), and they form eight sparse map sequences. All observations were carried out with the C_90 filter.

The scientific aim of the observing program was to carry out far-infrared measurements for studying the unified model of quasars, blazars and active galaxies. The sources were selected from the B3 VLA survey (for details see the proposal abstract in the ISO Data Archive). These observations were not published yet according to the note in the ISO Archive. In our HPDP photometric catalogue we present the fluxes of 64 compact galaxies measured at 90μm.

2 Data processing

2.1 From ERD to AAP level

The measurements were interactively reduced with the Phot Interactive Analysis (PIA) Version 10.0 (Gabriel et al. 1997). From ERD to AAP level the data

Table 1: Overview of the sparse map processing steps.

Processing steps	Applied
ERD	
Ramp Linearization	√
Ramp Deglitching (2 threshold method)	√
SRD	
Reset Interval Correction	√
Dynamic Transient Correction	√
Dark Current Subtraction	√
Signal Linearization	√
Signal Deglitching	√
Drift recognition	–
Combine signals (SRD − > SCP) (bi-weight mean averaging method)	√
SCP	
Calculate responsitivities (linear interpolation between the two FCS measurements)	√
Convert signals to monochromatic flux densities per pixel per raster position	√
AAP	

were processed in the same way as described for another data set by Moór et al. (2003). Note that we applied a dynamic transient correction routine developed in a joint project of the ISOPHOT Centre of MPIA and Konkoly Observatory. This routine is not implemented in PIA V10.0 and is available as a stand-alone IDL procedure. The method fits the temporal signal evolution within a measurement by interpolating within a library of signal dependent transient curves and predicts the signal at t=128 seconds (for details see del Burgo et al. 2002). The transient correction method was applied after the reset interval correction at the SRD level. Each sparse-map observations is bracketed by two FCS measurements. We used a linear interpolation in time between their responsivity values to calibrate the sparse map sequence. The applied data reduction and calibration steps were actually the same as we used and tested for mini-map observations in a previous HPDP product (see Moór et al. 2003). An overview of the processing steps of the sparse map data reduction is given in Table 1.

2.2 Creation of pseudo-AAP sequences

During a sparse map sequence the detector is continuously measuring, even during the slews between map positions, thus from a technical point of view a sparse map sequence resembles a PHT22 raster observation. This is even more true when at each sparse map position only one filter was used, like in the present compact galaxy case. Due to the technical similarities, we were inspired to adapt our flux extraction routines developed for mini-maps (Moór et al. 2003) for sparse-maps, too.

The PIA software yields AAP files as final products which contain the flux density and other data of a measurement. In order to produce an input imitating a mini-map, all AAP files belonging to a specific sequence of sparse-map observations was organized into a single IDL-structure we called 'pseudo-AAP'. A pseudo-aap contains only such measurements which were done with the same filter, and can be handled as if it was the AAP file of a normal ISOPHOT raster measurement.

2.3 Flux extraction from the pseudo-AAP

The compact galaxies in our sample were always positioned at the centre of the C100 camera (targets were observed by pixel #5 only) and the border pixels of the C100 detector provided sufficient information on the background level, thus it was possible to extract the source flux from the on-source measurement only. An alternative solution would have been to utilize the dedicated background measurements, but our tests demonstrated that for compact sources the former method is more optimal. Thus the dedicated background observations were only used to compute a flat-field array, which was applied on the on-source image. For each specific source measurement in the sparse map sequence a different flat-field array was derived via interpolation between the flat-field values computed from the individual background measurements.

After the flat-field correction the source flux was extracted from on-source measurement by fitting the measured beam profile (the fitting procedure was identical with the one developed for the mini-maps). We used a modified version of the PCASPHT method (Kiss & Klaas 2000) to extract the flux. The PCASPHT method is based on the fact that each pixel observes a certain amount of the flux of a central point source plus the background signal:

$$MEASURED_i = f_i \cdot SOURCE + BACKGROUND \tag{1}$$

We assume that the background is the same for all pixels. f_i is the footprint function which gives what fraction of the source flux is collected by pixel i (we used the measured beam profile). A simple linear fit to the measured fluxes as a function of f_i gives the flux density of the source (which is the slope of the fit) and the background value (which is the zero-point of the fit).

Finally it should be noted that the first measurements in a sparse map sequence turned out to be less reliable due to the non-stabilized signal (they are marked by a specific quality flag in the catalogue).

2.4 Spatial extent

Since the sources which are studied here are compact galaxies, we assumed in the processing that the targets are true point sources for ISOPHOT.

2.5 Empirical corrections

Our processing method was tested on similar sparse map observations of normal stars. All suitable normal star measurements were selected from the Archive, and fluxes for the stars were extracted as described in previous sections. A comparison of these measured fluxes with flux values predicted by photospheric models (for details see Moór et al. 2003) revealed no measurable systematic discrepancy in the final photometry, thus no empirical photometric correction – unlike in the case of mini-maps – was applied on the sparse map data.

2.6 Error budget

Formal flux uncertainty values were provided by the IDL procedure which fitted the measured fluxes of the different pixels as a function of the footprint values (the LINFIT routine in our case). The resulting flux errors range from $\sim$20 mJy to $\sim$70 mJy, with a median of 28 mJy. Since the majority of the compact galaxies turned to be undetected (see below), the standard deviation of their flux distribution should also provide an independent estimate of the typical measurement error. In our case a robust standard deviation computation gave 30 mJy for the dispersion of the measured galaxy fluxes around a mean value of -1 mJy, thus we can conclude that the flux uncertainty values provided by the LINFIT routine are reasonable.

2.7 Processing of the compact galaxy sample

The observations included to this catalogue were selected as was described in Section 1.2 and includes all compact galaxy observations proposed by M. Vigotti. At first, these observations were processed with PIA V10.0 including the steps given in Table 1, and at the SRD level we applied the transient correction described in Section 2.1. Pseudo-AAPs were formed (see Section 2.2) for each sequence and the flux extraction was carried out via the way outlined in Section 2.3.

The main results are given in the catalogue. The format of the catalogue can be found in the Appendix.

3 Examples

2 of the 64 sources has a higher detection level that 2σ. The highest flux density belongs to B3 1447+400 which has $F = 87$ mJy. The SEDs of two of examples are presented in Figures 1-2.

4 The catalogue

The description of the content of the catalogue can be found in the Appendix. The catalogue itself can be downloaded from the ISO Archive homepage.

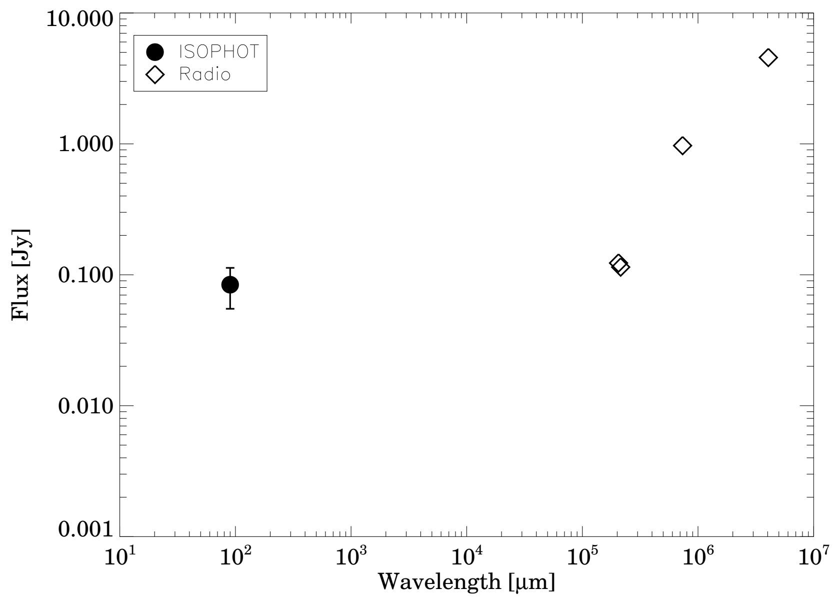

Figure 1: *SED of the radio-source B3 1447+400.*

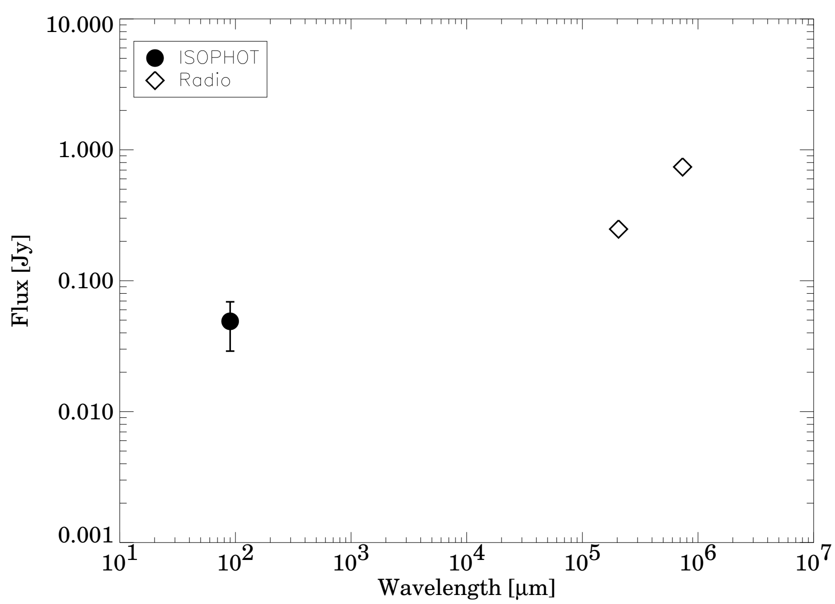

Figure 2: *SED of the radio-source B3 1356+397.*

References

del Burgo, C., Héraudeau, P., & Ábrahám, P. Exploiting the ISO Data Archive. Infrared Astronomy in the Internet Age, held in Siguenza, Spain 24-27 June, 2002. Edited by C. Gry, S. Peschke, J. Matagne, P. Garcia-Lario, R. Lorente, & A. Salama. Published as ESA Publications Series, ESA SP-511. European Space Agency, 2003, p. 339.

Gabriel C., Acosta-Pulido, J., Heinrichsen, I., et al., 1997, in Proc. of the ADASS VI conference (Eds.: G. Hunt, H.E. Payne, ASP Conf.Ser. 125), 108

Kiss Cs., Klaas, U., 2000, "General Re-validation of Point Source Photometry from PHT22 Mini-maps", ISOPHOT internal report

Moór, A., Ábrahám, P., Kiss, Cs., Csizmadia, Sz., 2003, *Far-infrared observations of normal stars measured with ISOPHOT in mini-map mode*, report on Highly Processed Data Products, Version 1.1, available on-line at the ISO Data Centre: *http://pma.iso.vilspa.esa.es:8080/hpdp/technical_reports/ technote38.html*

5 APPENDIX: description of the catalogue

The 'Catalogue of far-infrared measurements of compact galaxies measured in sparse-map mode with ISOPHOT' contains the measured fluxes at 90 microns of 64 extragalactic radio-sources determined by the above described procedure. The total number of all processed TDTs in this catalogue is 139 because of the sky background measurements.

The catalogue contains the following data:

Column	Field	Unit	Description
(1)	Object name		SIMBAD compatible name
(2)	Object type		Standard SIMBAD code for object type.
(3)	ISO name		Object name given by the ISO observer.
(4)	TDTNUM_ON		The 8-digit TDTNUM of the on-source observation.
(5)	On_ Meas.		Index of the on-source measurement within TDTNUM_ ON.
(6)	RA(2000)		Right ascension, h:m:s.
(7)	Dec(2000)		Declination, d:m:s.
(8)	Detector		ISOPHOT detector.
(9)	Wavelength	[micron]	Nominal wavelength of the ISOPHOT filter.
(10)	Aperture	[arcsec]	Aperture for detectors, square for C100
(11)	Epoch		Epoch of the observation.
(12)	TDTNUM_ OFF		The 8-digit TDTNUM of the off-source observation.
(13)	Off_Meas.		Index of the off-source measurement within TDTNUM_OFF.
(14)	Flux density	[Jy]	Flux density of the source. No colour correction applied.
(15)	Flux uncertainty	[Jy]	Flux uncertainty. No colour correction applied.
(16)	Background	[MJy/sr]	Background surface brightness. No colour correction applied.
(17)	Quality		Quality of the observation. R1 – Standard processing according to the scheme described in the report. R2 – Observation was carried out at the very beginning or at the very end of orbit. Reduced photometric reliability at orbital phase lesser than 0.2. R3 – The first measurement in a sparse map sequence generally less reliable due to the non-stabilized signal.

Table 2: Description of the catalogue